International Research Journal of Engineering and Technology (IRJET) e-ISSN: 2395-0056
Volume: 06 Issue: 01 | Jan-2019 www.irjet.net p-ISSN: 2395-0072

Three Dimensional Finite Element Analysis of Isolated Reinforced Concrete Footing on Sub-grade Soil

Ranajay Bhowmick[1]

[1]*Assistant Engineer, Public Works Department, Government of West Bengal, India*

Abstract - *Over the years Researchers have preferred to study the behaviour of reinforced concrete structures by carrying out experimental works. With the advent of Finite Element Method (FEM) and present day Finite Element Analysis (FEA) softwares, researchers have now become inclined to explore the area of numerical simulations to study the behaviour of reinforced concrete structures. The experimental investigation of the behaviour of isolated reinforced concrete column footing laid on deformable subgrade subjected to concentrated load has been very rare due to the complexity of the problem. As Finite element analysis using engineering softwares is increasingly used in modelling of different structures and in analysing their behaviour, an attempt has been made to study the behaviour of isolated reinforced concrete column footing laid on deformable subgrade and loaded by concentrated load until failure using FEA software ANSYS. Example problems from the experiments carried out in the past by researchers have been selected for the numerical simulation. Three-dimensional geometric modelling of the reinforced concrete footing along with the soil strata has been carried out. Suitable material models for concrete, reinforcement and soil have been chosen for the analysis. A comparative study, using combinations of different material models, have been carried out to determine the most suitable combination of material models for concrete, reinforcement and soil that would give results which matches well with the experimental results.*

Key Words: (ANSYS; cracking; FEA; footing; material model; reinforced concrete; soil)

1. INTRODUCTION

Reinforced Foundations resting on soil subgrade give rise to an interesting situation where there is interaction between two materials i.e. reinforced concrete and soil. Soil's characteristics in relation to reinforced concrete structures are completely different particularly in terms of deformability. Researchers over the years have dedicated their attention for studying the behavior of structural elements lying above ground, both experimentally and analytically. However, the behavior of structural elements, especially isolated reinforced concrete footing, below ground level is very scarcely studied experimentally primarily due to the complicated organization of such experiments and higher material costs. As investigations in real soil are rare and expensive, in many experiments real conditions are simulated by steel springs (car springs are used to simulate the soil behaviour) [Richart et al. (18), Talbot (22)] or by set of small hydraulic jacks connected in parallel and applying the load keeping the test specimen upside down [Hegger et al. (13,14,15), Simoes et al. (21), Urban et al. (24)] or by line loads which produce the same effect as the load exerted by a uniformly reactive soil [Timm (23), Hallgren (10,12)]. Very few researchers have carried out in situ experiments on reinforced concrete footings subjected to concentric loading. There are some tests in which footings are tested in a box of sand [Hegger (13,14,15)] or clay and sand in situ [Rivkin (19)]. Hegger et al (13,14,15) carried out several experiments on reinforced concrete column footings supported realistically by soil kept within a box (sand-box) of fixed dimensions to investigate the punching shear failure of footings when subjected to concentric external load. Very recently Bonic et al, Martina et el and Shill et al. (20) carried out experiments on in-situ soil. Bonic et al (6,25) carried out several experiments between 2009 to 2014 to determine behaviour of isolated reinforced concrete column footings resting on subgrade soil and loaded by external load until their failure. They constructed complete foundation structure in situ, consisting of prepared subgrade soil with prescribed geotechnical characteristics and column footings with proposed dimensions and defined characteristics of the concrete and the reinforcement. They observed that a higher degree of loading was required for footing failure when tested in situ. In another similar investigation Martina et al (16) tested reinforced concrete slabs in situ by applying concentric loading until failure. They found out that the real values of shear resistance were two times more than the values calculated as per Eurocode.

Another method of studying the physical response of the structural components to the system of external forces is the Finite Element Analysis. In recent years, the use of finite element analysis has increased due to the progress in knowledge and the increase in capabilities of computer software and hardware. It has now become the choice method to analyse reinforced concrete structural components. It is important that the numerical models should be based on reliable test results and also experimental and numerical analyses should complement each other in the investigation of a particular structural phenomenon. However, the application of FEA in analysing the response of the reinforced concrete footing subjected to concentric loading is very rare. Only very recently Bonic et al and Cajka et al carried out three-dimensional finite element analyses to validate their experiments on reinforced concrete footing on soil subgrade. Cajka et al (7) took several experimental measurements of reinforced concrete slab – subsoil

interaction and compared the results with numerical analysis by means of FEM. Their analyses were based on the concept that the concentration of vertical stress in the axis of the foundation differs from the homogeneous half-space and the static Young's modulus varies smoothly with depth. The soil – structure interaction was modelled using contact elements and the friction between soil and structure was neglected. They observed that when 3D elements are used for 3D tasks, the final deformation is considerably influenced by the size of the modelled area that represents the subsoil and also by the boundary conditions. The influence of any boundary condition becomes weaker with the increasing ground plan of the subsoil. Bonic et al (6) carried out three dimensional non-linear analyses to study the behaviour of reinforced concrete column footing laid on deformable subgrade and subjected to concentrated load until failure using software package ANSYS. The soil structure interaction was modelled using contact elements.

Therefore, it is essential that more efforts are made to study the behavior of reinforced concrete footing on soil subgrade by conducting real life in situ tests. It is also essential to determine suitable numerical simulation procedures with proper geometric and material modeling which would properly reflect the behavior of such reinforced concrete footings subjected to concentric loading at in situ conditions.

2 RESEARCH SIGNIFICANCE

The main obstacle to finite element analysis of reinforced concrete structures is the difficulty in characterizing the material properties. Much effort has been spent in search of a realistic model to predict the behavior of reinforced concrete structures. Due mainly to the complexity of the composite nature of the material, proper modelling of such structures is a challenging task. In this study an approach has been made to prepare three dimensional finite element models of isolated reinforced concrete footings on soil sub grade subjected to concentric loading and carry out non-linear finite element analyses till failure using the FEA software ANSYS. The success of such numerical simulation depends on proper geometric and material modeling which would properly reflect the bahavior of such R. C. Footings. Suitable three-dimensional elements have been chosen for geometric modeling of concrete, reinforcement and soil and three-dimensional finite element models were prepared. A comparative study has been carried out where different combinations of material models for concrete, reinforcement and soil have been used for the three-dimensional non-linear finite element analysis. The consequences of changes in modeling are discussed and combination of material models that closely matched the experimental results has been considered as most suitable for such numerical simulation.

3 NUMERICAL SIMULATION

Reinforced concrete and soil both exhibit inelastic behavior at different stages of loading. Therefore it becomes essential to carry out a nonlinear finite element analysis and to carry out such analysis, development of proper geometric and material models for concrete, steel and soil is important. In the present study for the purpose of such numerical analysis the general-purpose FEA software ANSYS is used. Three dimensional finite element model of reinforced concrete footing on subgrade soil is prepared using suitable available elements and material models for concrete, reinforcement and soil and nonlinear analysis of the model subjected to concentric loading is carried out until failure. Owing to the symmetry of the structure and the load only $1/4^{th}$ of the structure consisting of reinforced concrete footing and soil subgrade has been modeled.

For concrete applications in general, hexahedral elements are found to be more stable and efficient in convergence than the tetrahedral elements (8). Therefore eight-noded isoparametric Solid 65 element, having translations at each node in x, y and z directions have been used for the modeling of concrete. This element allows cracking at tension, crushing at compression, plastic behaviour and creep. A discrete approach, using two-noded three-dimensional isoparametric Link element having translations in x, y and z directions at each node, has been adopted for the modeling of reinforcements. A total adhesion between reinforcement and concrete and complete strain compatibility between the reinforcement elements and the concrete elements has been assumed. For the modeling of soil eight-noded isoparametric Solid 45 element, having translations in x, y and z directions at each node have been used.

Concrete is a heterogeneous and quasi-brittle material. The study of the stress-strain characteristics of plain concrete under uniaxial loading indicates that concrete behaves linearly up to about 30 percent of its maximum compressive strength (9). Above that stress level concrete begins to soften, due to the growth of bond cracks and as the mortar cracks start developing with the bond cracks growing further, the stress-strain curve shows a gradual increase in curvature up to about 75-90 percent of the maximum compressive strength. The curve approaches the peak as the bond and mortar cracks bridge together to form the zones of internal damages. Beyond the peak the curve has a descending part until crushing failure occurs at some ultimate strain. The response of reinforced concrete on external loading is complex and after reaching a certain amount of elastic deformation, elasto-palstic behavior is observed and finally failure may be caused due to several possible mechanisms such as concrete cracking, reinforcement yielding, bond slip between steel and concrete, concrete crushing etc.

ANSYS proposes the use of William-Warnke five-parameter model with the Solid 65 element for the modeling of brittle materials like concrete. ANSYS also provides option of combining William-Warnke five parameter model with any of several other nonlinear material models such as Kinematic Hardening Model, Isoparametric Hardening Model, Anisotropic Model, Drucker-Prager Model, Nonlinear Elasticity Model and Multilinear-Elastic Model. The William-

Warnke model was developed in 1974 and this model gives good agreement with the experimental results in the domain of working stress. In our present study the William-Warnke model has been combined with the Multilinear Elastic model. Steel is a ductile material, which after yielding strain-hardens sufficiently due to considerable plastic deformation before finally reaching failure. Therefore, the nonlinearity of reinforcement behavior is modeled using the elasto-plastic Bilinear-Kinematic Hardening model available in ANSYS. Soil is a granular material and essentially a disperse system in which particles are in a fine state of sub-division or dispersion. For modeling of such material ANSYS proposes the use of the elastic-perfectly-plastic Drucker-Prager model. In the present study Drucker-Prager model is used for the material modeling of the soil.

Table 1 - Summary of Material Model Combinations Analyzed

Analysis	Concrete Model		Reinforcing Steel Model		Soil Model
	Tension	Compression	Representation	Material Model	Material Model
A	Cracking	Linear Elastic + Crushing	Discrete	Linear Elastic	Linear Elastic
B	Cracking	Linear Elastic + Crushing	Discrete	Linear Elastic	Drucker-Prager
C	Cracking	Linear Elastic + Crushing	Discrete	Bilinear Kinematic	Drucker-Prager
D	Cracking	Multilinear Elastic	Discrete	Bilinear Kinematic	Drucker-Prager
E	Cracking	Multilinear Elastic + Crushing	Discrete	Bilinear Kinematic	Drucker-Prager
F	Cracking	Multilinear Isotropic + Crushing	Discrete	Bilinear Kinematic	Drucker-Prager

These material models of concrete, steel and soil are combined in different ways and these different combinations [Table 1] are used for the analysis of each of the example problems.

In the first combination linear behaviour of soil, steel and concrete has been assumed with concrete being capable of cracking in tension and crushing in compression. In the second combination an elastic-perfectly plastic model based on Drucker-Prager yield criteria has been used for soil whereas linear behaviour of steel and concrete has been assumed with concrete being capable of cracking in tension and crushing in compression. In the third combination linear behaviour of concrete has been assumed with concrete capable of cracking in tension and crushing in compression, but for steel Bilinear-Kinematic Hardening model has been used and the elastic-perfectly plastic model based on Drucker-Prager yield criteria has been used for soil. As for the fourth combination the concrete compressive behaviour is modeled using a Multilinear Elastic stress-strain model with concrete capable of cracking in tension and the Bilinear Kinematic Hardening model and the elastic-perfectly plastic model based on Drucker-Prager yield criteria are used respectively for steel and soil. In the fifth combination the concrete compressive behaviour is modeled using a Multilinear Elastic stress-strain model with concrete capable both of cracking in tension and crushing in compression and the Bilinear Kinematic Hardening model and the elastic-perfectly plastic model based on Drucker-Prager yield criteria are used respectively for steel and soil. In the sixth and final combination the concrete behaviour is modeled using Multilinear Isotropic Hardening model with concrete capable of both cracking in tension and crushing in compression and the Bilinear Kinematic Hardening model and the elastic-perfectly plastic model based on Drucker-Prager yield criteria are used respectively for steel and soil. These material model combinations are used to analyze example problems selected from experiments carried out in the past by researchers. The results of the analyses are then compared with experimental results. Results of the material model combination that has good agreement with the experimental results has been considered the most suitable combination for modeling.

The numerical procedure involved geometric modeling of the reinforced concrete column, footing and soil and carrying out nonlinear finite element analysis. In the geometric modeling, complete strain compatibility has been assumed between the reinforcement and the concrete elements. In the geometric model the mesh density of the reinforced concrete foundation is kept considerably higher than that of the soil block. As a result the two meshes are non-conforming. However, complete strain compatibility between concrete [Solid 65] and soil elements [Solid 45] at corresponding nodes has been assumed and the numerical analysis has been carried out without any contact modeling, using available contact elements, at the soil-structure interface.

The boundary conditions have been applied by providing suitable restraints to the nodes. The nodes at the bottom of the soil block have been restrained for translations in x-, y- and z-directions and the nodes on all vertical sides of the soil block have been restrained for translations perpendicularly to their sides in x- and z-directions. Nodes on the symmetry planes of concrete and soil block had restrained translations perpendicularly to the symmetry planes i.e. in x- and z-direction. The load has been applied at the top nodes of the column as concentric load directed downward and in increments of smaller load value until the failure load is reached. The solution scheme has

been the Newton-Raphson iterative scheme with a force based convergence criteria.

4 NUMERICAL EXAMPLES

Two test specimens, selected from the experiments carried out in the past by researchers, have been modeled and three-dimensional nonlinear finite element analyses have been carried out to observe the behavior of the specimens under concentric loading and the results of the analyses are then compared with the test results.

4.1.1 Hegger et al tested 10 reinforced concrete footings realistically supported by sandy soil in a box with fixed dimensions. The concrete compressive strength of the footings ranged between 20 – 40 MPa. From among those experiments DF1 has been chosen for analysis. The reinforced concrete footing DF1 was a square one (900 mm x 900 mm) with a square column (150 mm x 150 mm) on top of it. The property details of the footing tested are summarized in Table 2 and the test set up used is shown in Fig 1. The dimensions and reinforcement arrangements are given in Fig 2.

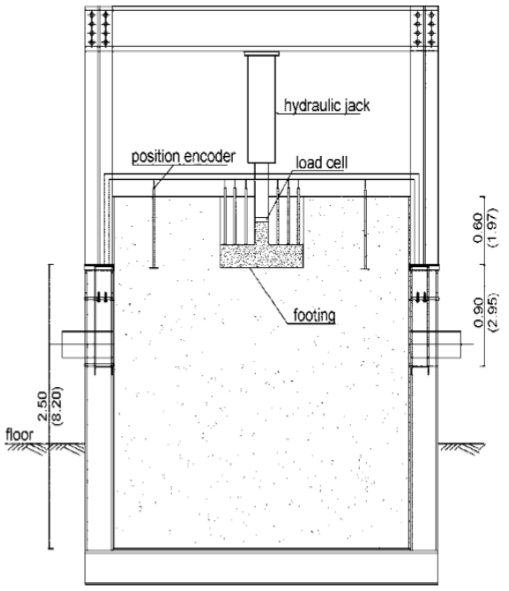

Fig 1 – Schematic Representation of the Test Set-up

Table 2 – Details of the Test Specimen

Footing no	d (mm)	c (mm)	a/d	fc,cyl (Mpa)	Ec (Gpa)	Est (Gpa)	Bar size	Es (Mpa)
DF1	150	150	2.5	20.2	24.0	210	14	44.2

Notes: d = effective depth of footing; c = width of column; fc,cyl = cylinder compression strength; Ec = Young's modulus of concrete; Est = Young's modulus of steel; Es = modulus of elasticity of soil

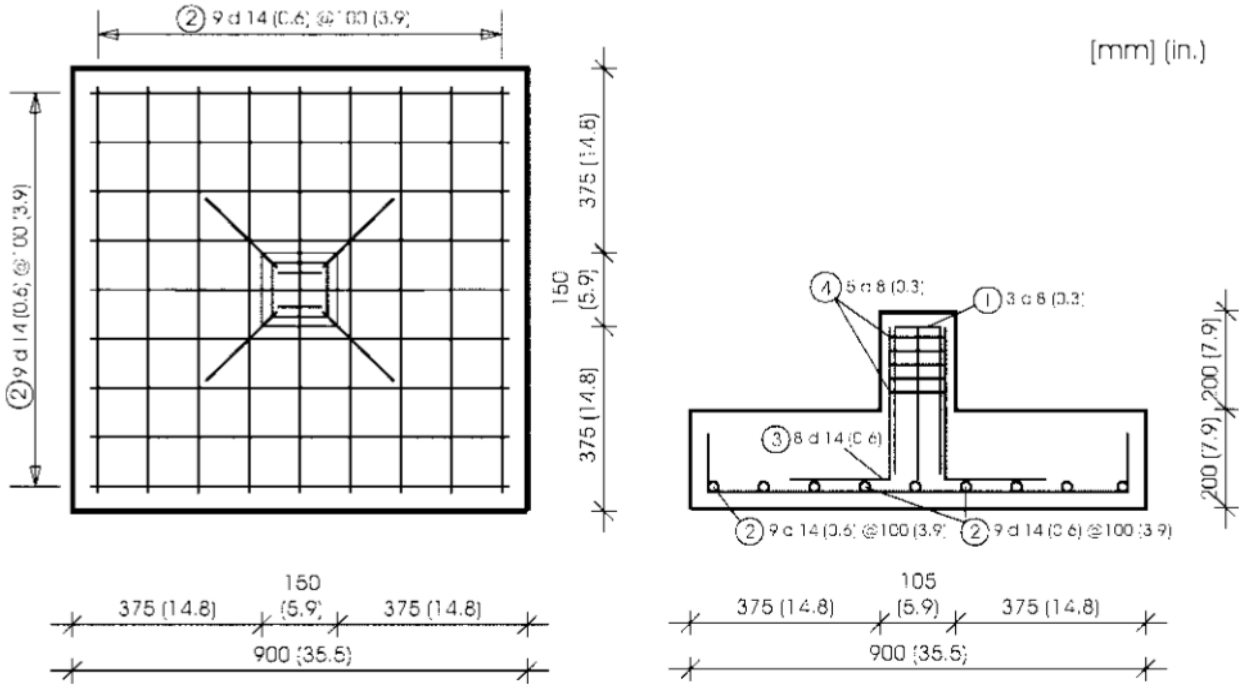

Fig 2 – Dimensions and Reinforcement arrangement of Footing DF1

4.1.2 NUMERICAL SIMULATION OF THE TEST SPECIMEN

For the purpose of analysis 1/4th of the complete experimental set up has been modeled. As has already been discussed the concrete and soil have been modeled using 8-noded isoparametric Solid 65 elements and 8-noded isoparametric Solid 45 elements respectively. The reinforcements have been modeled using 2-noded three dimensional isoparametric Link elements. Complete strain compatibility has been assumed between the reinforcement and the concrete elements and the concrete and soil elements. The finite element mesh is shown in the Fig 3.

A total of 12543 nodes, 3464 concrete elements, 302 steel elements and 5736 soil elements have been used in the finite element mesh of the column. The material properties of concrete, steel and soil used, for the analyses, are summarized in Table 3. After applying proper boundary conditions, as discussed before, load is applied in the form of nodal loads at the top of the column. The load has been increased gradually from 0 to 500 kN. The analysis has been carried out using the Newton-Raphson iteration method. A force based convergence criteria has been specified. These material models are combined in different ways and solutions are carried out for each of the different combinations. The combinations are referred here as DF1-A, DF1-B, DF1-C, DF1-D, DF1-E & DF1-F.

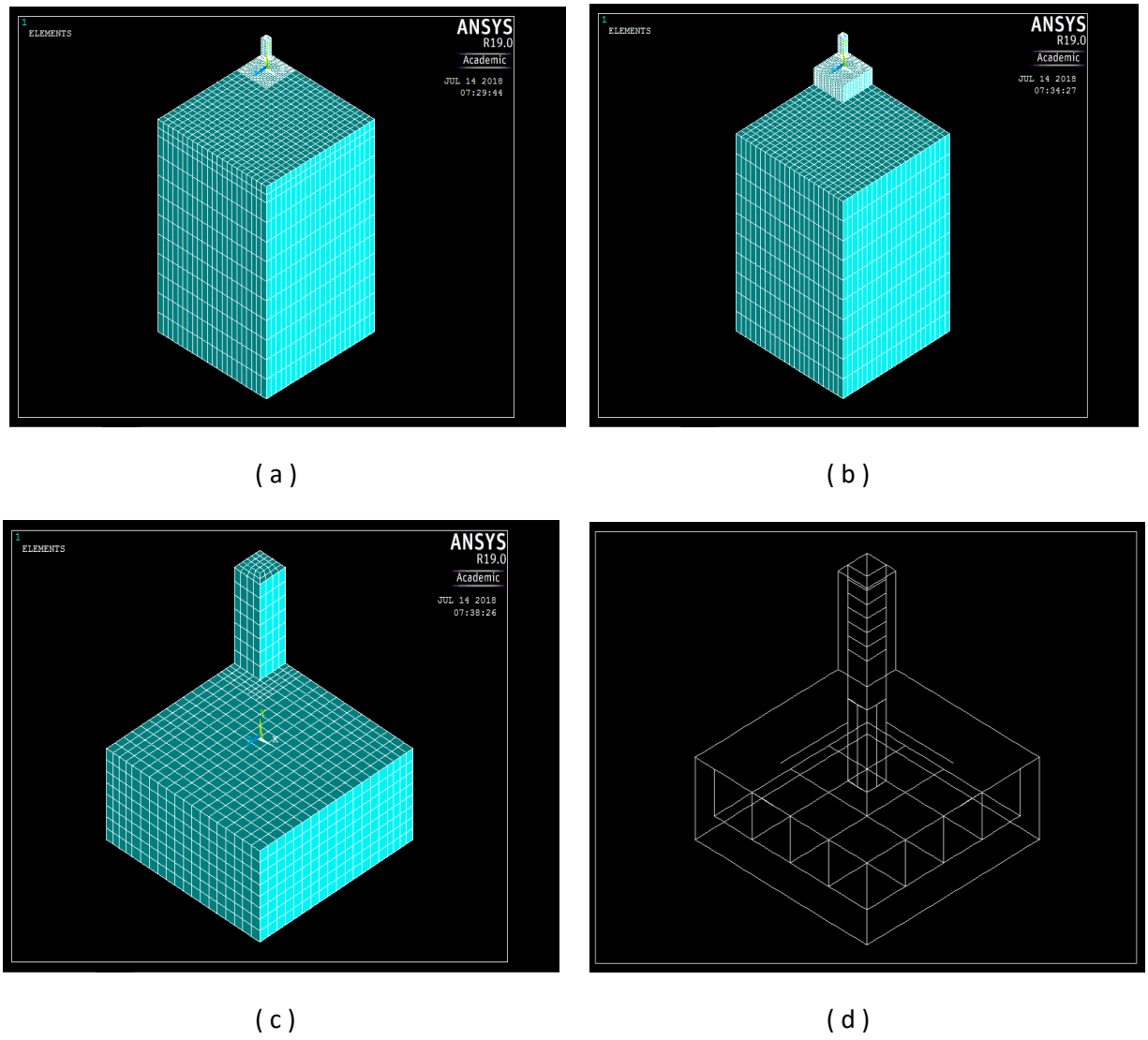

(a) (b)

(c) (d)

Fig 3 a) Complete Mesh of Footing & Soil b) Mesh without Top Soil c) Meshed Footing d) Reinforcement Arrangements

Material	Property						
	Linear		Non-Linear				
Concrete	Modulus of Elasticity (Mpa)	24000	Multilinear Isotropic Hardening/ Multilinear Elastic			Five-Parameter Model	
	Density (kN/m3)	25	Strain (ec)	Stress (fc) (Mpa)		Open Shear Transfer Co-efficient	0.3
				Coulmn	Footing		
			0.0001	3.15	2.38		
			0.0003	9.4	6.94		
	Poisson's Ratio	0.2	0.0005	15.38	11.00	Closed Shear Transfer Co-efficient	1.0
			0.0007	20.91	14.43		
			0.001	28.01	18.37		
			0.0012	31.81	20.25		
			0.0014	34.81	21.63	Uniaxial Cracking Stress (Mpa)	3.41
			0.0016	37.05	22.59		
			0.0018	38.59	23.22		
			0.002	39.53	23.59		
			0.0021	39.79	23.69	Uniaxial Crushing Stress (Mpa)	23.74
			0.0022	39.95	23.74		
			0.0023	40.00	23.76		
			0.0024	39.95	23.74		
			0.0025	39.82	23.70	Biaxial Crushing Stress (Mpa)	28.49
			0.003	38.30	23.15		
			0.0035	35.93	22.31		
			0.004	33.29	21.35	Hydrostatic Pressure	1.0
			0.0045	30.69	20.38		
			0.005	28.25	19.44		
			0.006	24.04	17.72	Hydrostatic Biaxial Crushing Stress (Mpa)	34.42
			0.007	20.67	16.25		
			0.008	17.99	14.99		
			0.009	15.84	13.91	Hydrostatic Uniaxial Crushing Stress (Mpa)	40.95
			0.01	14.09	12.99		
			0.02	6.26	7.99		
			0.03	3.83	5.93	Tensile Crack Factor	1.0
			0.05	2.06	4.06		
			0.07	1.37	3.15		
			0.1	0.88	2.40		
Steel	Modulus of Elasticity (Mpa)	210000	Bi-Linear Kinematic HardeningS				
	Density (kN/m3)	78.5	Yield Stress (Mpa)		570		
	Poisson's Ratio	0.3	Tangent Modulus of Elasticity (Mpa)		21000		
Soil	Modulus of Elasticity (Mpa)	44	Drucker – Prager Model				
			Cohesion		0.0001		
	Density (kN/m3)	20	Friction Angle		36		
	Poisson's Ratio	0.27	Dilatancy Angle		20		

Table 3 – Material Properties of Concrete, Steel and Soil for DF1

4.1.3 RESULTS AND DISCUSSIONS

For The experiments on the isolated footing were carried out by Hegger et al. to study the punching failure of the footing. During the experiments vertical displacements of the center and corner of the footing were noted and load-deflection curves were plotted [Fig 4a]. Similar load-deflection curves have been obtained from the finite element analyses carried out for six different combinations of the material models and their plots are given in Fig 4b & Fig 4c. The loads and the corresponding deflections just before failure are tabulated and given in Table 4. From the Table and the figures it can be observed that combination DF1-D gives the closest match to the experimental results in respect to the failure load obtained [the failure load from the combination DF1-D is 636.4 kN and that obtained from the experiment is 551 kN]. The deflection values are also closely matched by the combination DF1-D to the experimental results. The load and deflection values obtained from the analyses using the other material model combinations do not match well to the experimental results. It can be easily observed that the load deflection curves progress closely at the early stages of the loading and as the cracking starts they distances from each other. This indicates that the load-deflection behavior is influenced by the crack development pattern. Also the gradients of the curves are very steep until failure indicating that the footings maintained rigidity until failure, which is a typical phenomenon for punching failure.

In their experiment Hegger et al. made measurements to determine the distribution of the concrete strain along radius of the slab. Since the strain distribution at the top of the slab is not a reliable indicator for the real stress distribution in the compression zone, the compressive strains inside the slab are measured and plotted [Fig 5a]. The strain plot indicates that the level of strain is higher near the edge of the column. Similar plots of radial concrete strains have been obtained from the finite element analyses and that of the combination DF1-D is presented here [Fig 5b]. The comparison of the two sets of plots indicates a clear similarity between them. The maximum strain level at failure obtained from experiment had been 3.0 % whereas the strain level just before failure has been approximately 0.6 % and at failure has been about 6.5 % for the finite element analysis.

Hegger et al. also made measurements to determine the soil pressure distribution underneath the footing and the plots of the soil pressure distribution at failure is given in Fig 6a. Similar observations have been made in the finite element analyses and the plots of the soil pressure distributions at failure are presented in the Fig 6b. The stress levels obtained from the experiments vary between 0.6 – 0.8 Mpa whereas that from the analysis of the combination DF1-D varies between 0.5 – 0.7 Mpa. Therefore, the comparison of the plots shows that the results of the combination DF1-D is the closest to the experimental results than the results obtained from other combinations.

A study of the development of the cracking in concrete at different stages of loading is made in the analyses and that for the combination DF1-D is represented in the Fig 7. The crack development patterns at different stages of the loading are shown for the complete footing and the base layer of the footing for different load levels. As the load level increases cracking starts from the central region of the base of the footing and as load levels increases more and more cracks get spread throughout the base of the footing and also the depth of the footing and column.

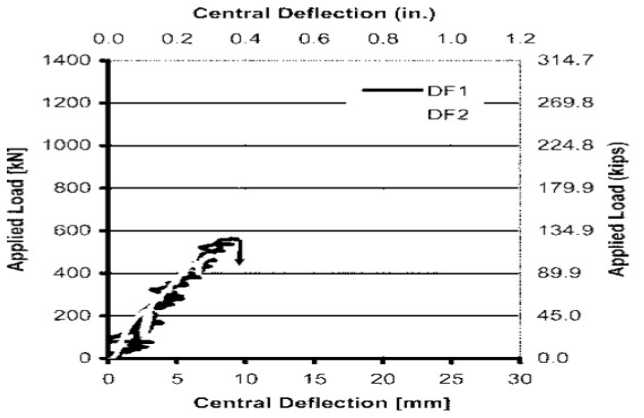

Fig 4a – Load-Deflection Curves obtained from Experiment

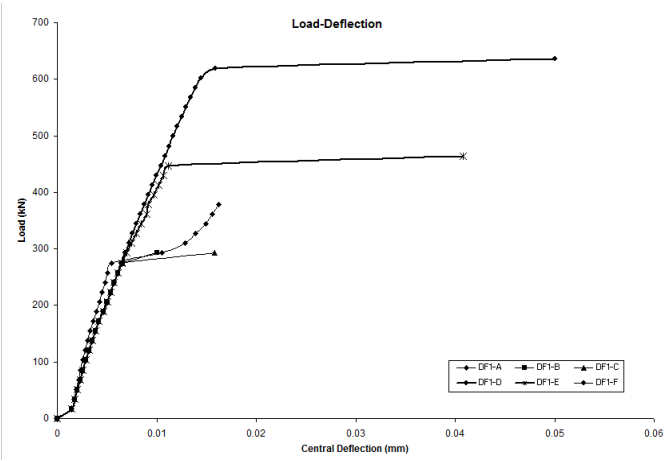

Fig 4b – Load-Deflection Curves obtained from Analyses for Center of Footing

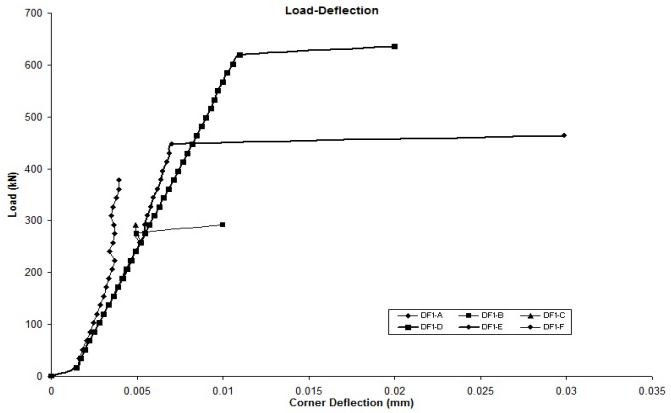

Fig 4c - Load-Deflection Curves obtained from Analyses for Corner of Footing

Table 4 – Failure Loads and Corresponding Deflection values

Combination	Load at Failure (kN)	Central Deflection just before Failure (mm)	Corner Deflection just before Failure (mm)
Experiment	551	10	-
DF1-A	378.4	16.25	3.928
DF1-B	292.4	6.57	4.99
DF1-C	292.4	6.57	4.99
DF1-D	636.4	15.881	10.99
DF1-E	464.4	11.16	7.06
DF1-F	240.8	5.75	4.92

* Since the final deflections, corresponding to the failure loads, found from the analyses are extremely large values, the deflection values just before failure are represented here.

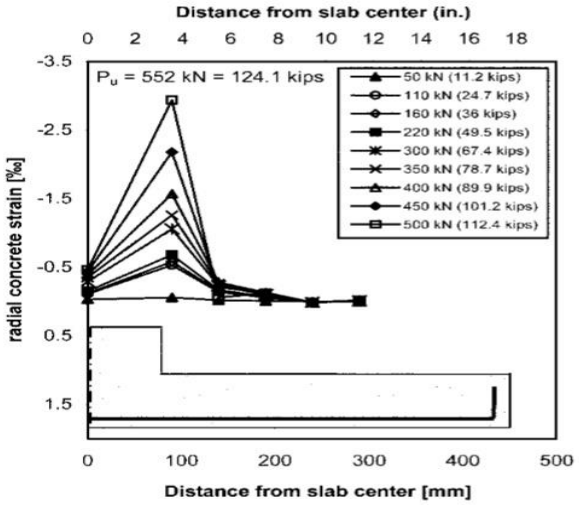

Fig 5a – Concrete Strain Distribution in Radial Direction obtained from Experiment

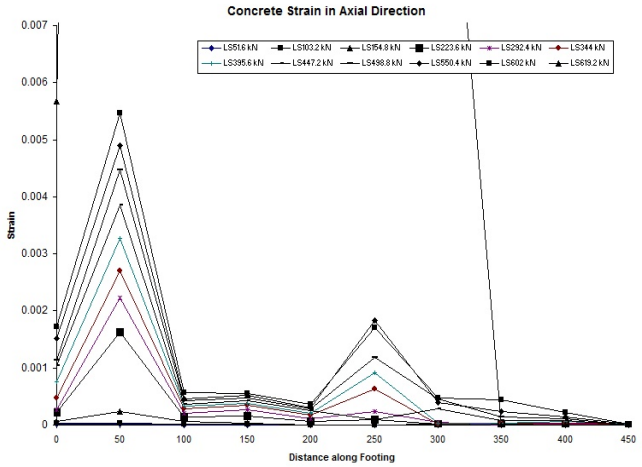

Fig 5b - Concrete Strain Distribution in Radial Direction just before failure obtained from Analyses

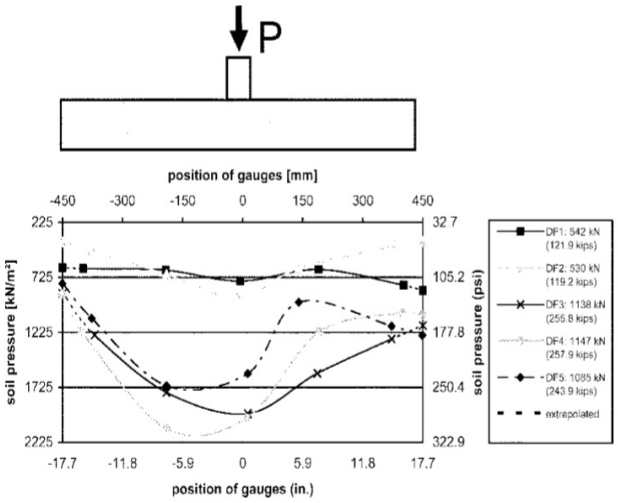

Fig 6a – Soil Pressure Distribution Close to Failure obtained from Experiment

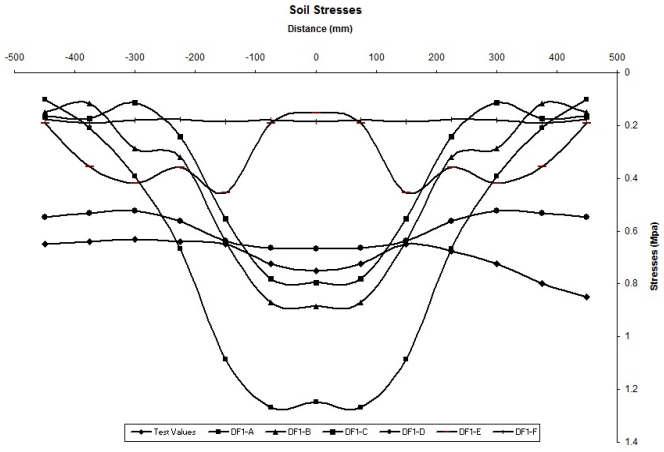

Fig 6b - Soil Pressure Distribution Close to Failure obtained from Analyses

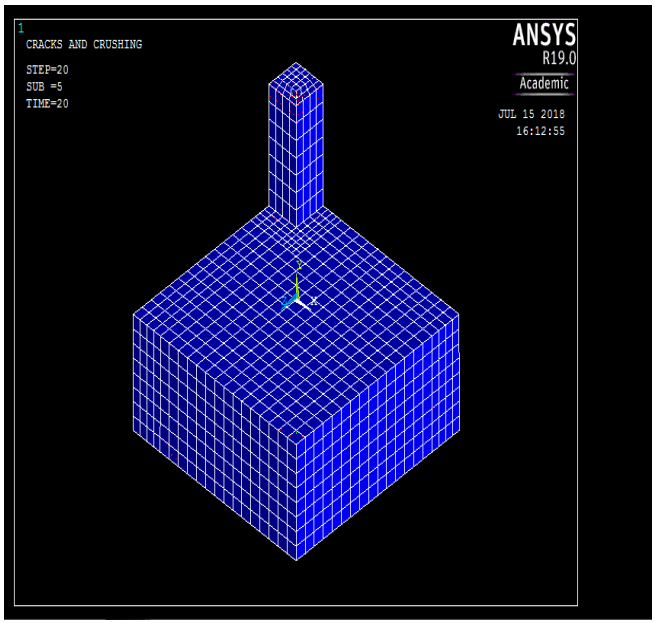
1
CRACKS AND CRUSHING
STEP=20
SUB =5
TIME=20
ANSYS
R19.0
Academic
JUL 15 2018
16:12:55

(a)

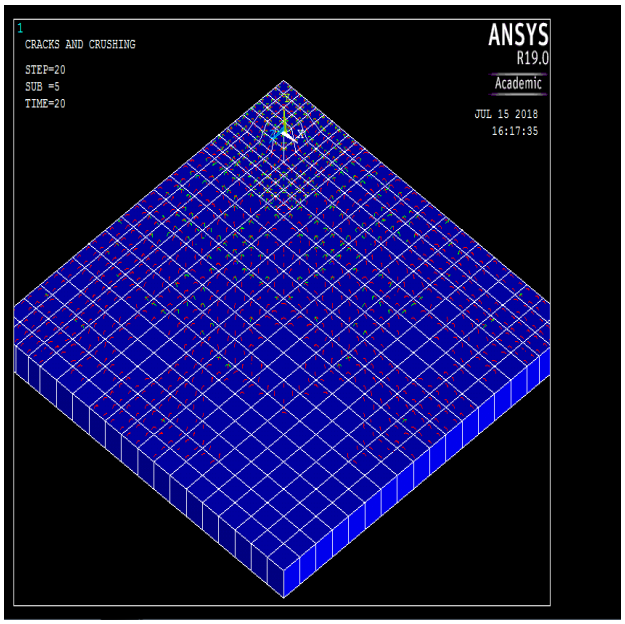
1
CRACKS AND CRUSHING
STEP=20
SUB =5
TIME=20
ANSYS
R19.0
Academic
JUL 15 2018
16:17:35

(b)

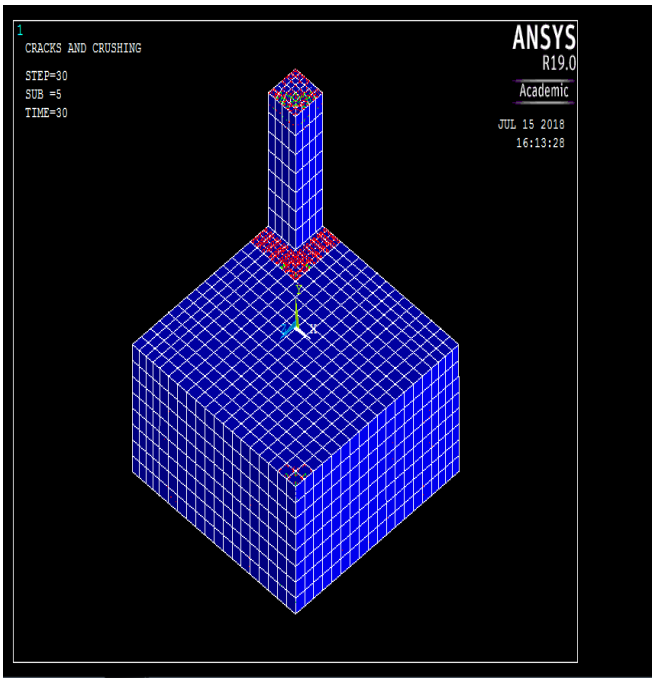
1
CRACKS AND CRUSHING
STEP=30
SUB =5
TIME=30
ANSYS
R19.0
Academic
JUL 15 2018
16:13:28

(c)

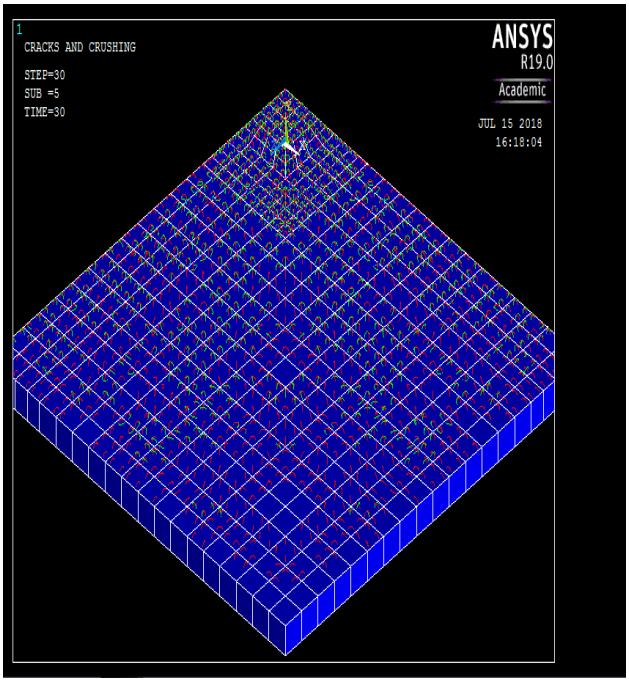
1
CRACKS AND CRUSHING
STEP=30
SUB =5
TIME=30
ANSYS
R19.0
Academic
JUL 15 2018
16:18:04

(d)

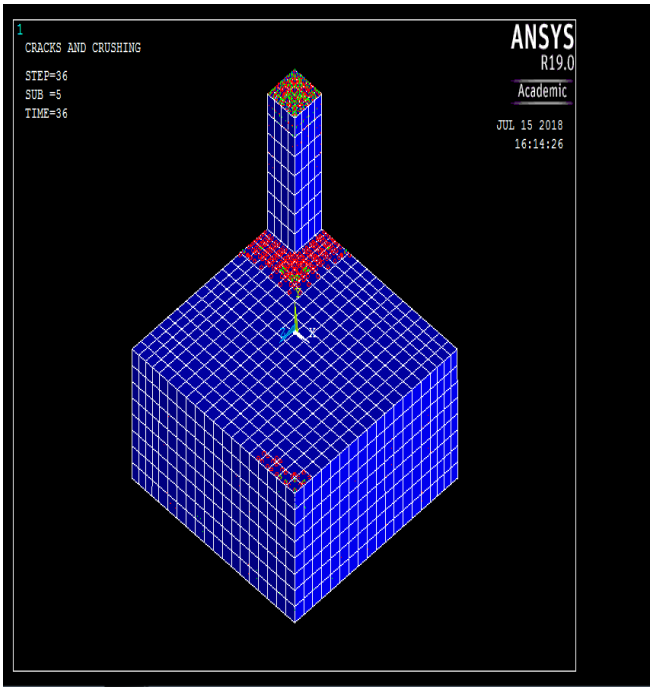

(e)

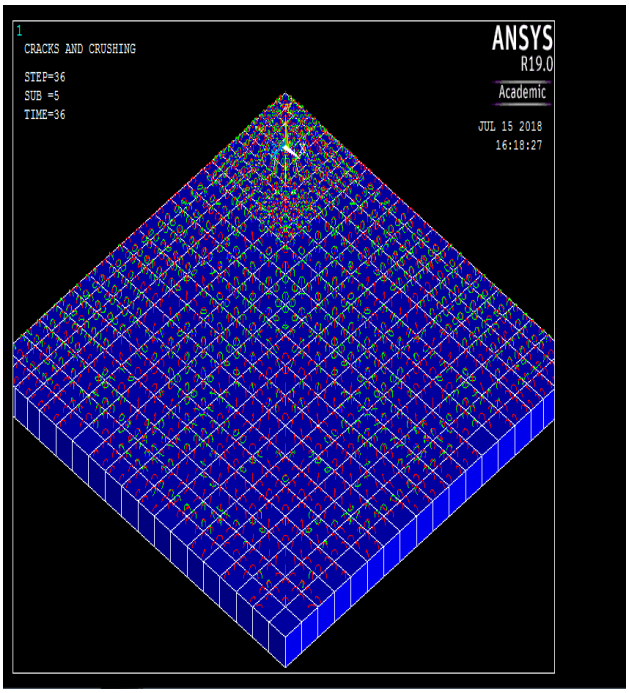

(f)

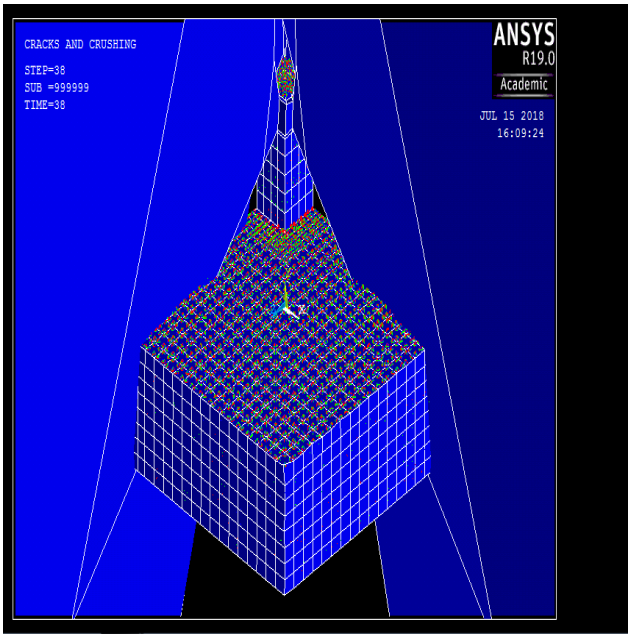

(g)

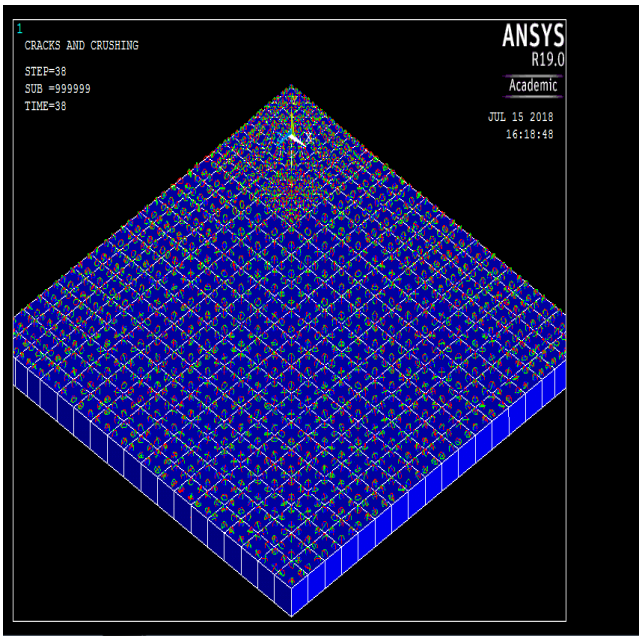

(h)

Fig 7 (a, b, c, d, e, f, g, h) – Development of Cracks at different Stages of Loading

4.2.1 Bonic et al tested 12 reinforced concrete footings supported by prepared sub grade soil. The experimental analyses were carried out by constructing the complete foundation structure in situ. From among those experiments TIX has been chosen for analysis. The tested reinforced concrete footing TIX was a square one (850 mm x 850 mm) with a square column (175 mm x 175 mm) on top of it. The property details of the footing tested are summarized in Table 5 and the test set up used is shown in Fig 8a. The dimensions and reinforcement arrangements are given in Fig 8b.

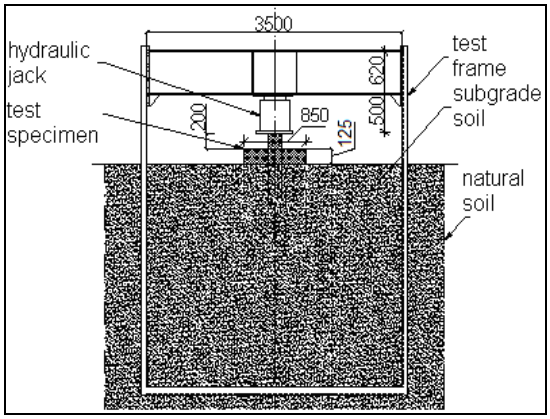

Fig 8 (a) Schematic Representation of the Test Set-up and Loading Arrangement

Table 5 – Details of the Test Specimen

Footing no	d (mm)	c (mm)	fc,cyl (Mpa)	Ec (Gpa)	Est (Gpa)	Bar size	Es (Mpa)
TIX	100	175	20.2	28.91	210	8	40.0

Notes: d = effective depth of footing; c = width of column; fc,cyl = cylinder compression strength; Ec = Young's modulus of concrete; Est = Young's modulus of steel; Es = modulus of elasticity of soil

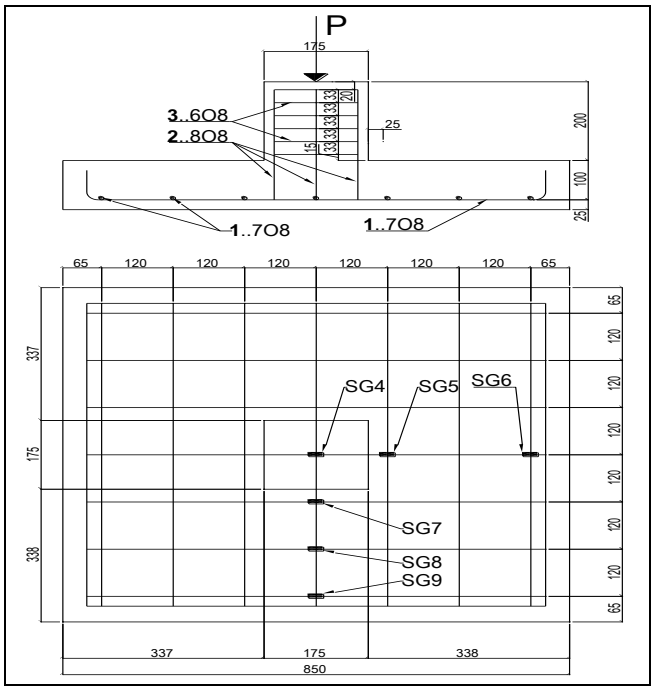

Fig 8 (b) Dimensions and Reinforcement arrangement of Footing TIX

4.2.2 NUMERICAL SIMULATION OF THE TEST SPECIMEN

For the purpose of analysis 1/4th of the complete experimental set up has been modeled. As has already been discussed the concrete has been modeled using 8-noded isoparametric Solid 65 elements and the soil has been modeled using 8-noded isoparametric Solid 45 elements. The longitudinal and transverse reinforcements have been modeled using 2-noded Link8 elements. Complete strain compatibility has been assumed between the reinforcement and the concrete elements and the concrete and soil elements. The finite element mesh is shown in the Fig 9. A total of 6652 nodes, 1309 concrete elements, 221 steel elements and 4000 soil elements have been used in the finite element mesh of the column. The material properties of concrete, reinforcement and soil are summarized in Table 6. After applying proper boundary conditions, as discussed before, load is applied in the form of nodal loads at the top of the column. The load has been increased gradually from 0 to 500 kN. The analysis has been carried out using the Newton-Raphson iteration method. A force based convergence criteria has been specified. These material models are combined in different ways and solutions are carried out for each of the different combinations. The combinations are referred here as TIX-A, TIX -B, TIX -C, TIX -D, TIX -E & TIX -F.

Table 6 - Material Properties of Concrete, Steel and Soil for TIX

Material	Property						
	Linear		Non-Linear				
Concrete	Modulus of Elasticity (Mpa)	28910	Multilinear Isotropic Hardening/ Multilinear Elastic			Five-Parameter Model	
	Density (kN/m3)	25	Strain (ec)	Stress (fc) (Mpa)		Open Shear Transfer Co-efficient	0.3
				Coulmn	Footing		
			0.0001	3.91	2.21		
			0.0003	11.71	6.35		
	Poisson's Ratio	0.2	0.0005	19.45	9.89	Closed Shear Transfer Co-efficient	1.0
			0.0007	26.99	12.78		
			0.001	37.56	15.94		
			0.0012	43.82	17.40		
			0.0014	49.21	18.44	Uniaxial Cracking Stress (Mpa)	3.13
			0.0016	53.57	19.15		
			0.0018	56.81	19.61		
			0.002	58.89	19.87		
			0.0021	59.52	19.94	Uniaxial Crushing Stress (Mpa)	20.0
			0.0022	59.88	19.98		
			0.0023	60.00	20.00		
			0.0024	59.88	19.98		
			0.0025	59.57	19.95	Biaxial Crushing Stress (Mpa)	24.0
			0.003	55.63	19.57		
			0.0035	49.56	18.97		
			0.004	43.07	18.30	Hydrostatic Pressure	1.0
			0.0045	37.06	17.61		
			0.005	31.82	16.94		
			0.006	23.71	15.69	Hydrostatic Biaxial Crushing Stress (Mpa)	29.0
			0.007	18.08	14.61		
			0.008	14.15	13.67		
			0.009	11.32	12.85	Hydrostatic Uniaxial Crushing Stress (Mpa)	34.5
			0.01	9.24	12.14		
			0.02	2.35	8.11		
			0.03	1.05	6.32	Tensile Crack Factor	1.0
			0.05	0.37	4.59		
			0.07	0.19	3.71		
			0.1	0.09	2.96		
Steel	Modulus of Elasticity (Mpa)	210000	Bi-Linear Kinematic HardeningS				
	Density (kN/m3)	78.5	Yield Stress (Mpa)		570		
	Poisson's Ratio	0.3	Tangent Modulus of Elasticity (Mpa)		21000		
Soil	Modulus of Elasticity (Mpa)	40	Drucker – Prager Model				
			Cohesion		0.0001		
	Density (kN/m3)	17	Friction Angle		40		
	Poisson's Ratio	0.27	Dilatancy Angle		20		

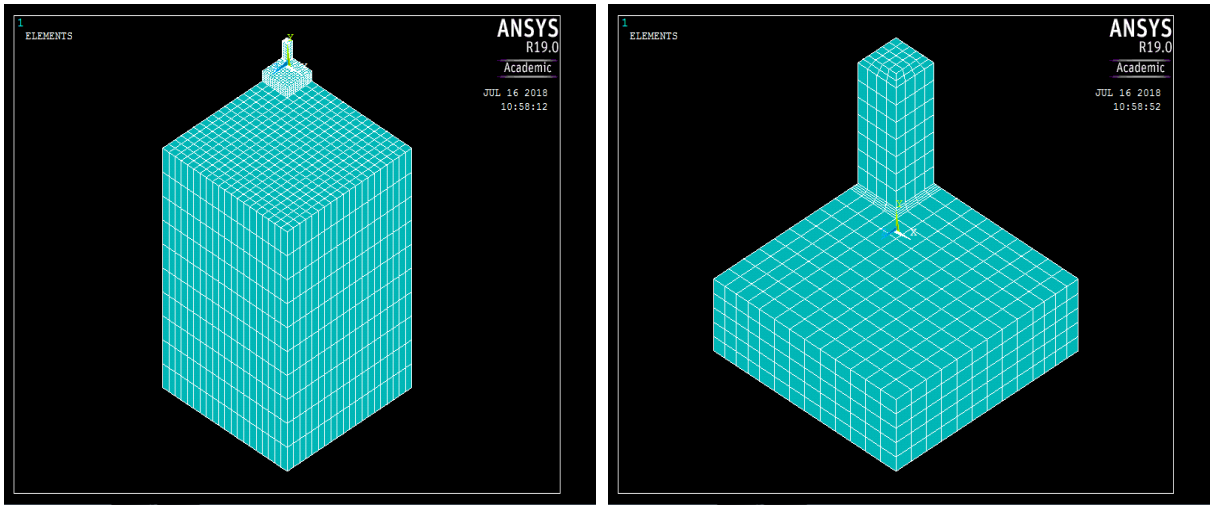

(a) (b)

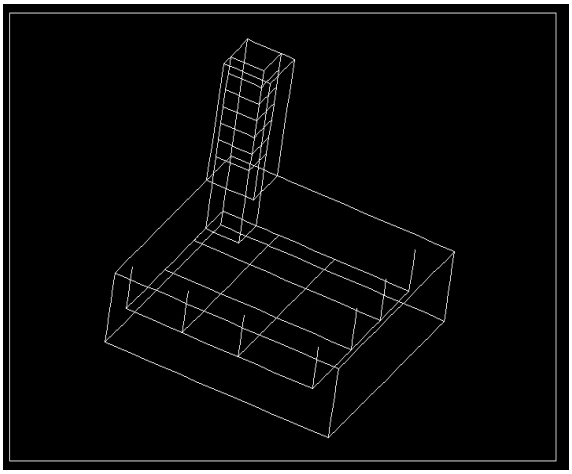

(c)

4.2.3 RESULTS AND DISCUSSIONS

Bonic et al. did experiments on isolated reinforced concrete footings and then carried out nonlinear finite element analyses to describe the response of footing when subjected to concentric loading. In the present study an effort has been made to find out the suitable model combination for nonlinear finite element analyses that would provide results, which would be in good agreement to the results obtained by Bonic et al. The load –deflection responses obtained by Bonic et al. is given in Fig 10a. It can be seen that the experimental load gradually increased from zero to a maximum value of 430 kN, whereas finite element analysis load increased from zero to a maximum of 500 kN. In the present study similar load-deflection curves have been obtained from nonlinear finite element analysis of six different combinations of material models and the results are plotted in Fig 10b. The loads and the corresponding deflections just before failure are tabulated and given in Table 7.

From the Table and the figures it can be observed that combination TIX-D gives the closest match to the experimental results in respect to the failure load obtained as the failure load from the combination TIX -D is 433.44 kN and that obtained from the experiment is 430 kN. The deflection values are also closely matched by the combination TIX -D to the experimental results. The load and deflection values obtained from the other material model combinations are not well matched to the experimental results. It can also be observed that initially the gradients of the curves are very steep and they progress closely, but as the cracking starts they diverge from each other.

Bonic et al. studied the overall course of development of crackings and crushings at several typical stages of loading. A similar study of the development of the cracking in concrete is made in the present analyses.

Table 7 - Failure Loads and Corresponding Deflection values

Combination	Load at Failure (kN)	Central Deflection just before Failure (mm)	Corner Deflection just before Failure (mm)
Experiment	430	29	7.7
FEA by Bonic	500	25.1	6.8
TIX-A	319.92	17.55	4.38
TIX -B	144.48	6.96	3.15
TIX -C	113.52	7.0	3.16
TIX -D	433.44	22.73	4.69
TIX -E	227.04	9.59	3.21
TIX -F	113.52	4.52	3.36

* Since the final deflections, corresponding to the failure loads, found from the analyses are very large values, the deflection values just before failure are represented here.

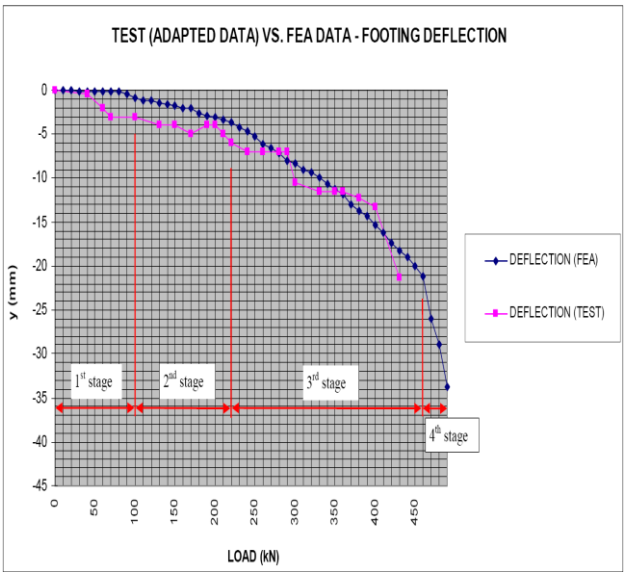

Fig 10a - Load-Deflection Curves obtained from Experiment

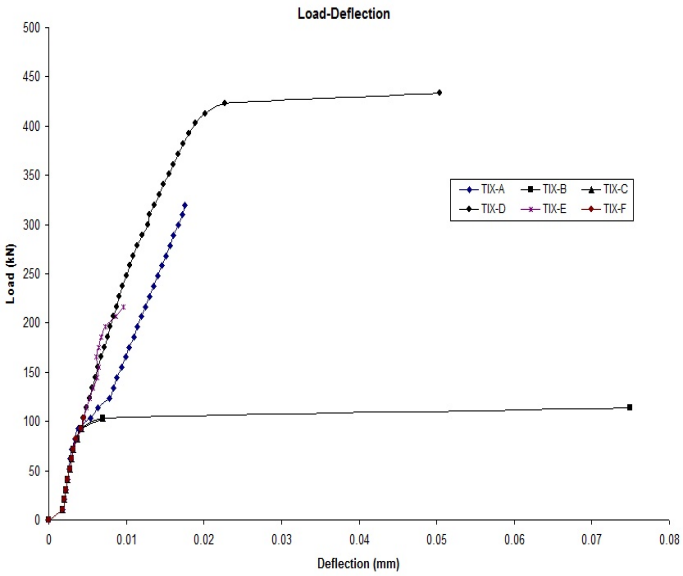

Fig 10b - Load-Deflection Curves obtained from Analyses

A comparison of the crack development pattern observed by Bonic et al. and that for the combination TIX-D (crushing in concrete is not allowed) has been made and presented in the Fig 11. The comparison reveals that for both the analyses the cracks start developing at the bottom layer of the footing below the column region and spreads throughout the base layer and then the whole footing and column. However, the rate of development of cracking for the combination TIX-D is slower than that of the analysis by Bonic et al.

Bonic et al. also studied the development of principal stresses in footing and column and a similar study has been made in the present analyses. A comparison of the development of principal stresses at different stages of loading is presented in Fig 12 and the similarity between them can be clearly observed.

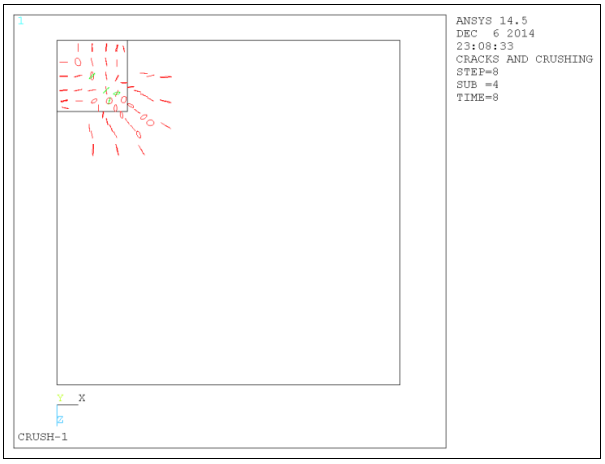
ANSYS 14.5
DEC 6 2014
23:08:33
CRACKS AND CRUSHING
STEP=8
SUB =4
TIME=8
CRUSH-1

(a)

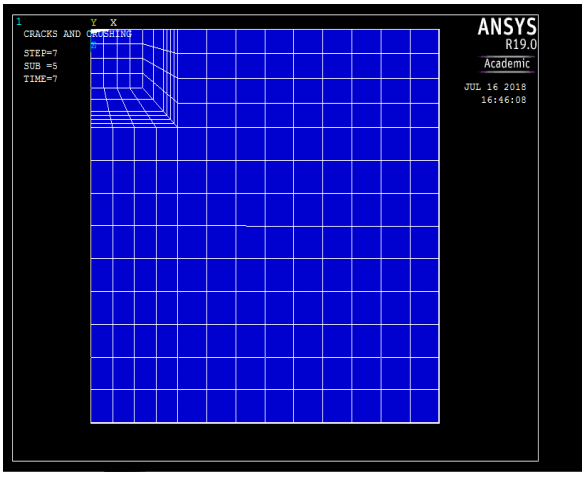
CRACKS AND CRUSHING
STEP=7
SUB =5
TIME=7
ANSYS
R19.0
Academic
JUL 16 2018
16:46:08

(b)

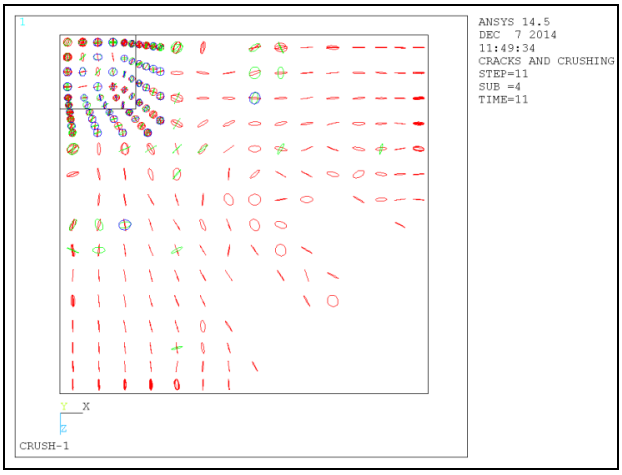
ANSYS 14.5
DEC 7 2014
11:49:34
CRACKS AND CRUSHING
STEP=11
SUB =4
TIME=11
CRUSH-1

(c)

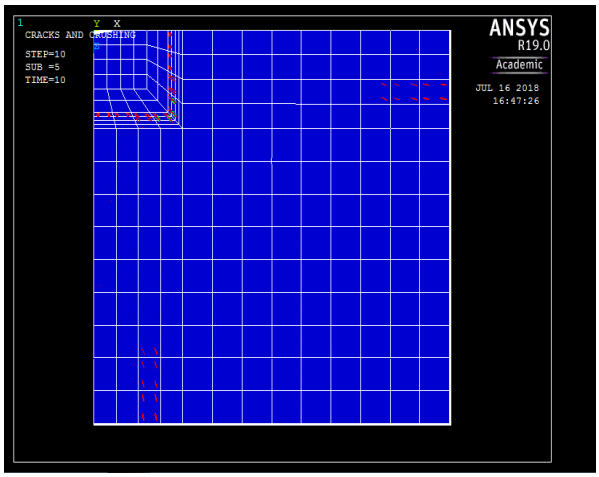
CRACKS AND CRUSHING
STEP=10
SUB =5
TIME=10
ANSYS
R19.0
Academic
JUL 16 2018
16:47:26

(d)

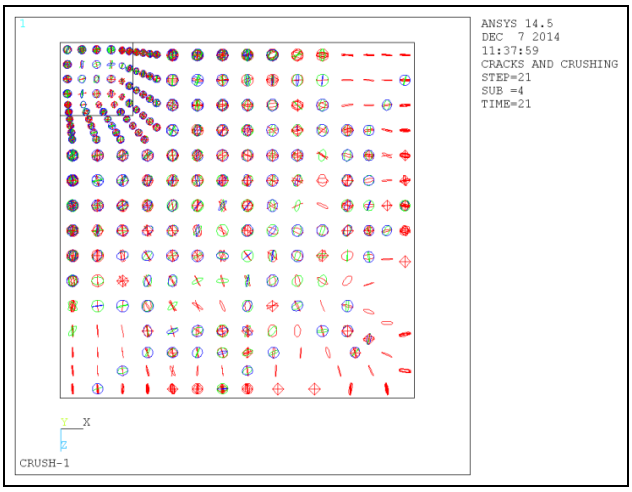
ANSYS 14.5
DEC 7 2014
11:37:59
CRACKS AND CRUSHING
STEP=21
SUB =4
TIME=21
CRUSH-1

(e)

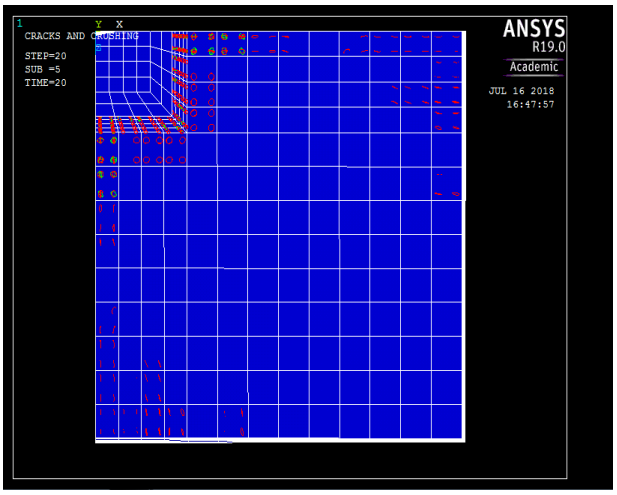
CRACKS AND CRUSHING
STEP=20
SUB =5
TIME=20
ANSYS
R19.0
Academic
JUL 16 2018
16:47:57

(f)

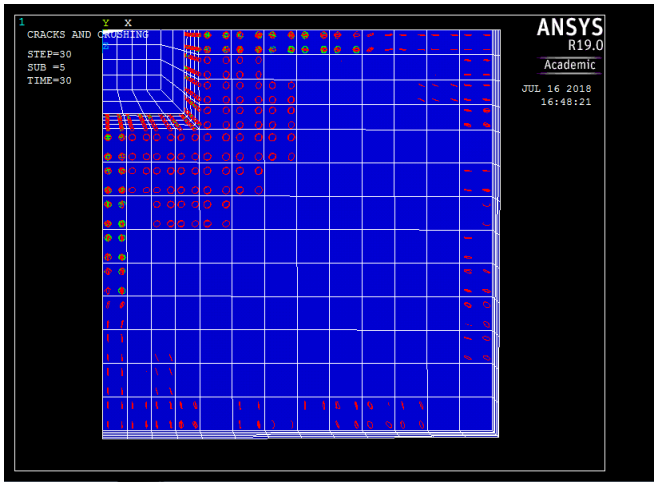

(g)

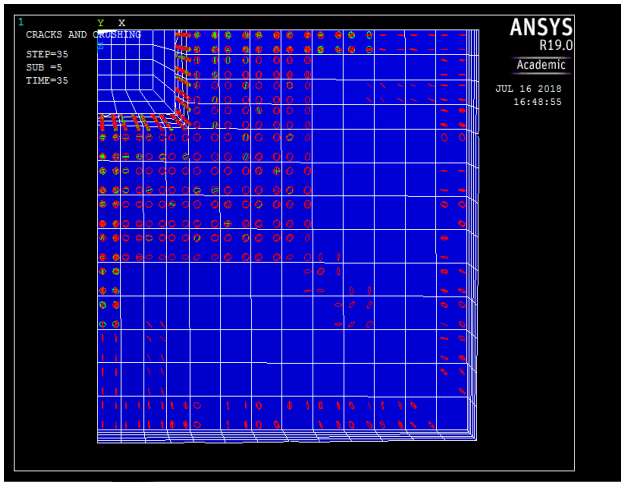

(h)

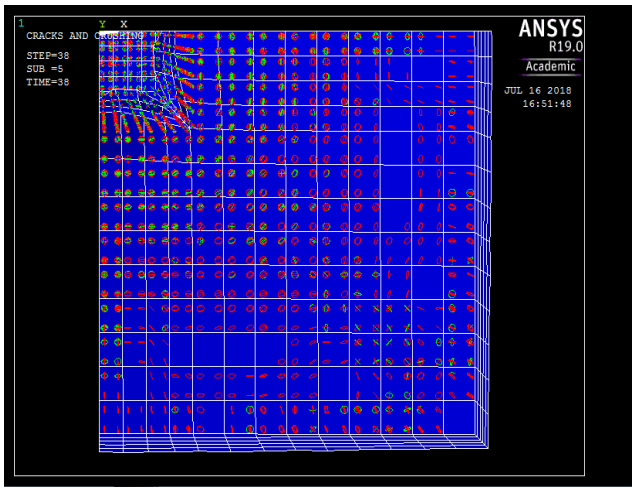

(l)

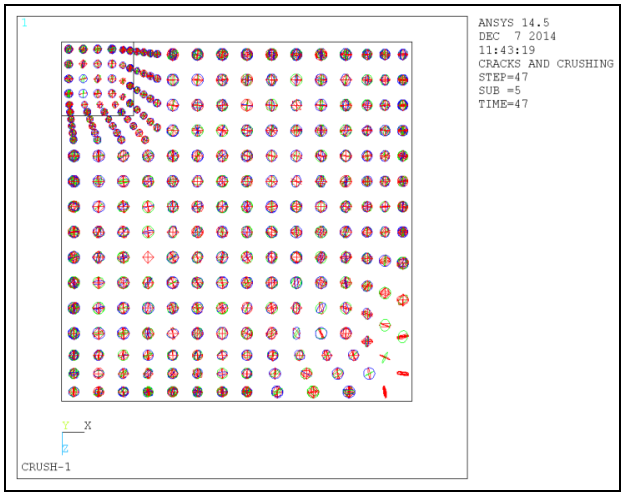

(j)

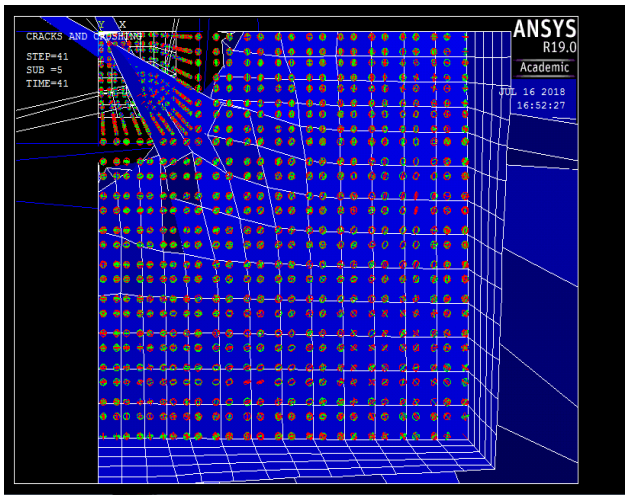

(k)

Fig 11 (a, c, e, j) – Development of Cracks at different stages of Loading for Bonic's Analysis

(b, d, f, g, h, i, k) – Development of Cracks at different stages of Loading for Present Study

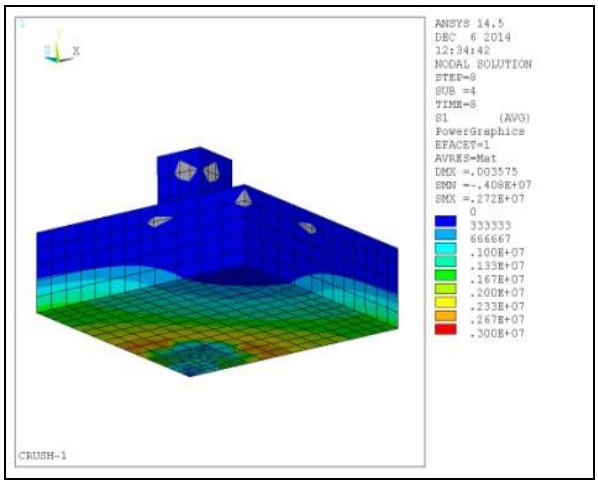
ANSYS 14.5
DEC 6 2014
12:34:42
NODAL SOLUTION
STEP=8
SUB =4
TIME=8
S1 (AVG)
PowerGraphics
EFACET=1
AVRES=Mat
DMX =.003575
SMN =-.408E+07
SMX =.272E+07
0
.333333
.666667
.100E+07
.133E+07
.167E+07
.200E+07
.233E+07
.267E+07
.300E+07
CRUSH-1

(a)

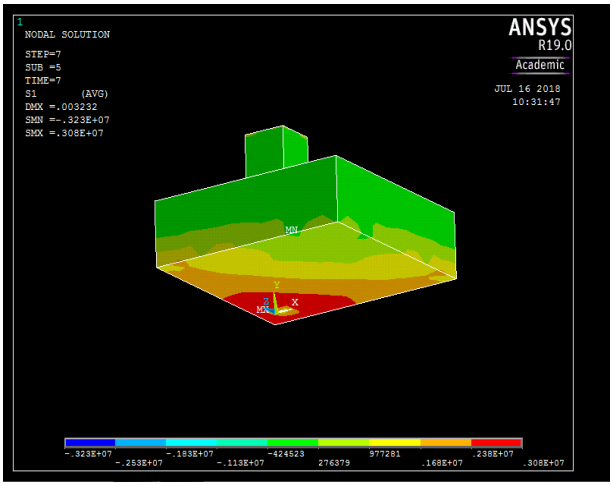
NODAL SOLUTION
STEP=7
SUB =5
TIME=7
S1 (AVG)
DMX =.003232
SMN =-.323E+07
SMX =.308E+07
ANSYS
R19.0
Academic
JUL 16 2018
10:31:47
-.323E+07
-.253E+07
-.183E+07
-.113E+07
-424523
276379
977281
.168E+07
.238E+07
.308E+07

(b)

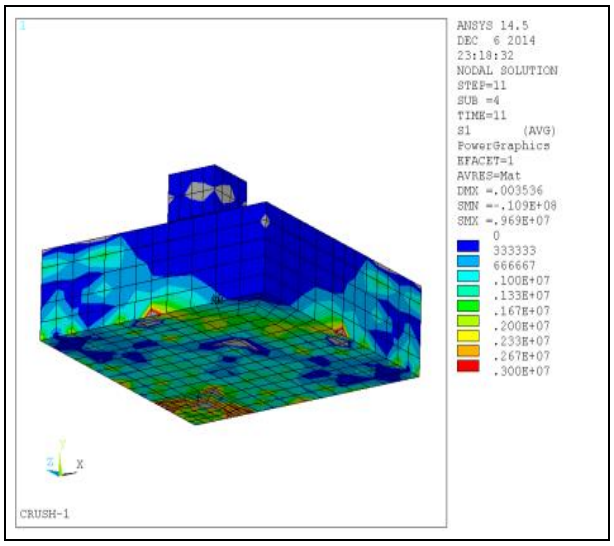
ANSYS 14.5
DEC 6 2014
23:18:32
NODAL SOLUTION
STEP=11
SUB =4
TIME=11
S1 (AVG)
PowerGraphics
EFACET=1
AVRES=Mat
DMX =.003536
SMN =-.109E+08
SMX =.969E+07
0
.333333
.666667
.100E+07
.133E+07
.167E+07
.200E+07
.233E+07
.267E+07
.300E+07
CRUSH-1

(c)

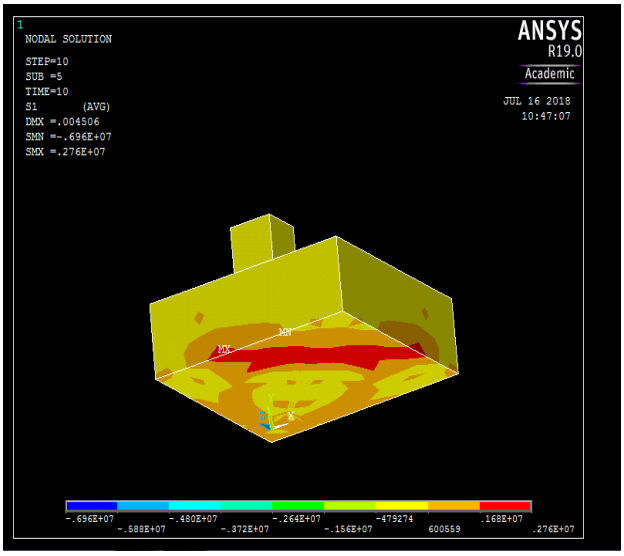
NODAL SOLUTION
STEP=10
SUB =5
TIME=10
S1 (AVG)
DMX =.004506
SMN =-.696E+07
SMX =.276E+07
ANSYS
R19.0
Academic
JUL 16 2018
10:47:07
-.696E+07
-.588E+07
-.480E+07
-.372E+07
-.264E+07
-.156E+07
-479274
600559
.168E+07
.276E+07

(d)

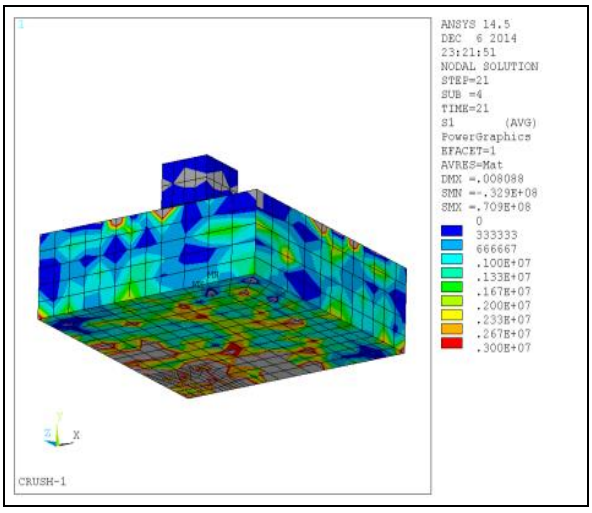

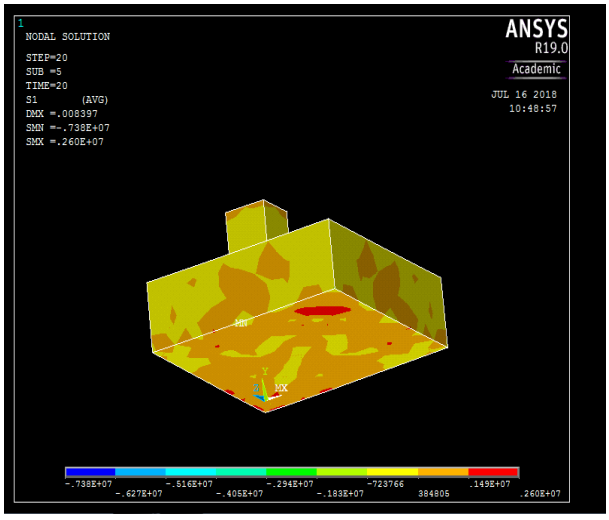

(e) (f)

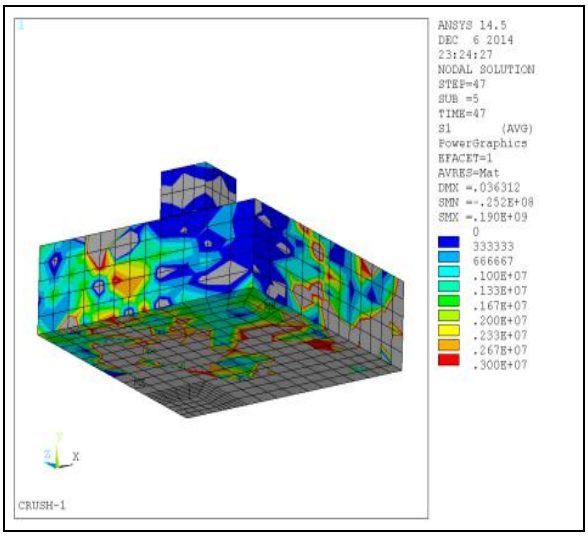

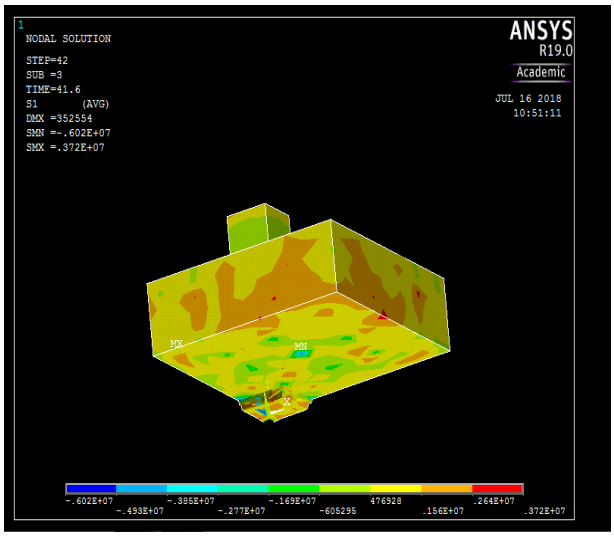

(g) (h)

Fig 12 (a, c, e, g) – Principal Stresses at different stages of loading in Bonic's Analysis
(b, d, f, h) – Principal Stresses at different stages of loading in the Present Study

5. CONCLUSIONS

The aim of the present study has been to find out the suitable material model combination from the material models available in ANSYS that can be successfully used for finite element analysis of foundation structure on subsoil, subjected to static loading, to obtain realistic solutions to the problem. Six different material model combinations have been selected for the finite element analyses and two experimental problems, chosen from the research works carried out in the recent past by Hegger et al. and Bonic et al., have been modeled and analyzed. The outcomes of the analyses have been similar for both the experimental problems in the sense that in each case the closest match to the experimental results have been obtained when the concrete compressive behaviour is modeled using a Multilinear Elastic stress-strain model with concrete capable of cracking in tension and the Bilinear Kinematic Hardening model and the elastic-perfectly plastic model based on Drucker-Prager yield criteria are used respectively for steel and soil. It has been possible to determine the entire load-deflection diagram and the ultimate load from such material model combination. It should also be noted that the modeling of the behavior of concrete has influenced the outcomes mostly rather than the modeling of the behavior of the other materials used. Concrete, a heterogeneous and quasi-brittle material, fails mainly due to the growth of mortar cracks and bond cracks. The failure of concrete in crushing occurs mainly when the concrete is subjected to triaxial compression. Therefore, it can be concluded that the failure of the foundation structures studied has been primarily due to the failure of concrete due to cracking and the material model combination mentioned above has been the most suitable amongst all selected.

REFERENCES

[1] ANSYS Software Documentation. Release 19.0 ANSYS, Inc. Canonsburg, PA. 2018.

[2] Barbosa, A. F. and Ribeiro, G. O. (1998), "Analysis of reinforced concrete structures using ANSYS nonlinear concrete model", Computational Mechanics, New Trends and Applications, S. Idelsohn, E. Oñate and E. Dvorkin (Eds.), ©CIMNE, Barcelona, Spain, pp 1 – 7.

[3] Bhargava, P., Bhowmick, R., Sharma, U. and Kaushik, S. K. (2004), "Three Dimensional Finite Element Modeling of Confined High Strength Concrete Columns", Proc. Int. Symp. On Confined Concrete, Changsha, China.

[4] Bhowmick, R. (2018), "Numerical Simulation of Isolated Reinforced Concrete Footing on Sub-Grade Soil", Proceedings of 9th International Conference on Contemporary Issues in Science, Engineering and Management, Dubai, pp. 04.

[5] Bonić, Z. (2011), "A contribution to the failure calculation theory by punching shear of column footings resting on deformable subgrade soil", PhD thesis, Faculty of Civil Engineering and Architecture, Niš, Serbia, pp. 182 (in Serbian).

[6] Bonic, Z., Davidovic, N., Vacev, T., Romic, N., Zlatanovic, E. and Savic, J. (2017), "Punching Behaviour of Reinforced Concrete Footings at Testing and According to Eurocode 2 and fib Model Code 2010", International Journal of Concrete Structures and Materials, 11(4), pp 657 – 676.

[7] Cajka, R. and Labudkova, J. (2013), "Influence of parameters of a 3D numerical model on deformation arising in interaction of a foundation structure and subsoil", Recent Advances in Urban Planning and Construction, pp 119 – 124.

[8] Chen, W. F. (1982), "Plasticity in Reinforced Concrete", McGraw-Hill, New York.

[9] Chen, W. F. and Saleeb, A. F. (1982), "Constitutive Equations for Engineering Materials", Vol.-I, Elasticity and Modeling, J. Wiley & Sons.

[10] Hallgren, M. (2000), "Non-Linear Finite Element Analyses of Column Footings Loaded to Punching Shear Failure", Proceedings of the International Workshop on Punching Shear Capacity of RC Slabs, Stockholm, pp. 75-82.

[11] Hallgren M. and Bjerke M. (2002), "Non-linear finite element analyses of punching shear failure of column footings", Cement & Concrete Composites, 24, p. 491–496.

[12] Hallgren M., Kinnunen S. and Nylander B. (1998), "Punching shear tests on column footings. Nordic Concrete Research", 21(1), p.1–24.

[13] Hegger J., Sherif A. G. and Ricker M. (2006), "Experimental Investigations on Punching Behavior of Reinforced Concrete Footings", ACI Structural Journal, 103(4), pp. 604-613.

[14] Hegger J., Ricker M., Ulke B. and Ziegler M. (2007), "Investigations on the punching behavior of reinforced concrete footings", Engineering Structures, 29, p. 2233–2241.

[15] Hegger, J., Ricker, M. and Sherif, A. G. (2009), "Punching strength of reinforced concrete footings", ACI Structural Journal, 106(5), pp 706–716.

[16] Martina, S., Pavlina, M. and Buchta, V. (2016), "Deformation of Foundation Structure and their Experimental Testing", International Journal of Theoritical and Applied Mechanics, 1, pp 303-308.

[17] Neville, A. M. and Brooks, J. J. (1994), "Concrete Technology", Longman Group Limited, England.

[18] Richart, F. E. (1948), "Reinforced Concrete Wall and Column Footings", ACI JOURNAL, Proceedings, 45, Part 1, No. 2, pp. 97-127; Part 2, No. 3, pp. 237-260.

[19] Rivkin, S. (1967), "Calculation of Foundations", Budivel'nik, (in Russian).

[20] Shill, S. K., Hoque, M. M. and Shaifullah, M. (2015), "Punching Shear Behavior of R C Column Footing on Stabilized Ground", International Journal of Engineering Technology, Management and Applied Sciences, 3 (Special Issue), pp 246 – 253.

[21] Simoes, J. T., Bujnak, J., Fernandez, R. M. and Muttoni, A. (2016), "Punching Shear Tests on Compact Footings with Uniform Soil Pressure", Structural Concrete, 4, pp 603 – 617.

[22] Talbot, A. N. (1913), "Reinforced Concrete Wall Footings and Columns under Concentrated Loads", Research and Development Bulletin, D47, Illinois.

[23] Timm, M. (2003), "Durchstanzen von Bodenplatten unter rotationssymmetrischer Belastung", PhD thesis, Institut für Baustoffe, Massivbau und Brandschutz, Technical University of Brunswick, Brunswick, Germany, pp 159, (in German).

[24] Urban, T., Goldyn, M., Krakowski, J. and Krawczyk, L. (2013), "Experimental Investigation on Punching Behavior of Thick Reinforced Concrete Slabs", Archives of Civil Engineering, 59(2), pp 157–174.

[25] Vacev, T., Bonic, Z., Prolovic, V., Davidovic, N. and Lukic, D. (2015), "Testing and finite element analysis of reinforced concrete column footings failing by punching shear", Engineering Structures, 92, pp 1 – 14.

[26] Zienkiewicz, O. C. and Taylor, R. L. (2000), "The Finite Element Method, Vol. 2: Solid and Structures, 5th edition Butterworth-Heinemann, Oxford.